Mammalian Biology
https://doi.org/10.1007/s42991-025-00546-3

ORIGINAL ARTICLE

Intraspecific differentiation and phylogeography of the Damaraland mole-rat *Fukomys damarensis* reveals rapid colonization of arid savannahs during the late Pleistocene

Radim Šumbera[1] · Michaela Uhrová[1] · Nigel C. Bennett[2] · Seth J. Eiseb[3,4] · Chris G. Faulkes[5] · Kyle T. Finn[6] · Matěj Lövy[1] · Ketty Phiri[7] · Paul A.A.G. Van Daele[1] · Barbora Zíková[1] · Ondřej Mikula[1,8]

Received: 28 February 2025 / Accepted: 12 November 2025

Abstract

The Damaraland mole-rat (*Fukomys damarensis*) is a cooperatively breeding rodent primarily inhabiting sandy soils of southern Africa. It has the largest distribution of all the species in the genus *Fukomys*, from northwestern South Africa to Zambia, and from central Namibia across to western Zimbabwe. To the north of the Zambezi River in Zambia, it is replaced by its sister species Micklem's mole-rat (*Fukomys micklemi*). Despite a long history of studying the species, phylogeography of *F. damarensis* remains poorly understood. We analysed its intraspecific genetic structure and past population trends using mitochondrial cytochrome *b* sequences (published as well as acquired from museum and newly collected specimens). Also, we explored major axes of soil and climate variation among localities inhabited by this species. For comparison, we performed the same series of analyses also for *F. micklemi*. Within *F. damarensis*, we identified three major matrilineages. They were all found together in the Upper Zambezi – Okavango Delta region, where their habitat characteristics overlap widely with those of *F. micklemi*. However, one of the matrilineages likely underwent rapid expansion southwards to the sandy soils of Botswana, Namibia and northwestern South Africa. The expansion was tentatively dated to the second half of the last glacial, a period of increasing aridity and formation of sandy soils. This is in sharp contrast to *F. micklemi*, whose population had been much more stable over the last glacial cycle.

Keywords Population expansion · Kalahari sands · Zambezi River · Aridity · Cooperative breeder

Communicated by: Susanne Holtze.

✉ Ondřej Mikula
onmikula@gmail.com

[1] Department of Zoology, Faculty of Science, University of South Bohemia, České Budějovice, Czech Republic

[2] Department of Zoology and Entomology, Mammal Research Institute, University of Pretoria, Pretoria, South Africa

[3] Department of Environmental Science, University of Namibia, Windhoek, Namibia

[4] Mammalogy Collection, National Museum of Namibia, Windhoek, Namibia

[5] School of Biological and Behavioural Sciences, Queen Mary University of London, London, UK

[6] Department of Biology and Environmental Science, Ecology and Evolution in Microbial Model Systems, Linnaeus University, Kalmar, Sweden

[7] Plot 4399, Kanjala Drive, Chipata City, Eastern Province, Zambia

[8] Institute of Vertebrate Biology, Czech Academy of Sciences, Brno, Czech Republic

Published online: 07 January 2026

Introduction

African mole-rats (Bathyergidae) are strictly subterranean rodents distributed across savannah habitats in sub-Saharan Africa (Bennett and Faulkes 2000). The family comprises approximately 30 species within six genera (Faulkes and Bennett 2021), although the species' limits are still far from being fully resolved (c.f. species lists in Happold 2013; Monadjem et al. 2015). Two species of mole-rats have received special attention due to their highly social lifestyle. The first is the naked mole-rat (*Heterocephalus glaber*, Rüppell, 1842) from the Horn of Africa, which is currently studied almost exclusively by laboratory approaches (see Buffenstein et al. 2021 for review). The second is the Damaraland mole-rat (*Fukomys damarensis*, Ogilby, 1838), a member of the genus *Fukomys* (northern common mole-rat), the most speciose bathyergid genus. Unlike *H. glaber*, *F. damarensis* has been extensively studied both in laboratory conditions and in the wild, including several medium- to long-term studies conducted at different sites (e.g., Jarvis and Bennett 1993; Fang et al. 2014; Young et al. 2015; Mynhardt et al. 2021; Wong et al. 2022; Thorley et al. 2023).

The Damaraland mole-rat has the largest and most southern distributional range of all species in the genus *Fukomys*. It occurs across southern Africa, including northwestern South Africa, northern and eastern Namibia, Botswana, western Zimbabwe, and southwestern Zambia (Bennett and Jarvis 2004; Happold 2013). Its distribution is most commonly associated with the Kalahari sands, where it occurs in arenosols and coarse sandy soils of arid and semi-arid thorn scrub acacia savannahs. At the northern edge of its range, *F. damarensis* is replaced by its sister species, *F. micklemi*. In this study, *F. micklemi* is delimited broadly, so it includes also populations referred to as *F. anselli* and *F. kafuensis* (Burda et al. 1999), as suggested by preliminary analyses of nuclear genomic data (Mikula et al. in prep). The presumed contact zone roughly follows the course of the Zambezi River, although in Zambia, *F. damarensis* occurs on both sides of the river (Van Daele et al. 2007).

Cytogenetically, *F. damarensis* is known to contain three chromosomal variants: 2n = 74, 2n = 78 and 2n = 80 (Nevo et al. 1986; Van Daele et al. 2004; Deuve et al. 2008), whereas its genetic variability remains poorly understood despite a long history of studying the species. The existing genetic data for *F. damarensis* come primarily from large-scale phylogenetic studies on African mole-rats, with very few individuals sampled from each site. According to the sequence divergence at mitochondrial cytochrome *b* gene, differences among populations of *F. damarensis* are small (Faulkes et al. 2004; Van Daele et al. 2007), even over large geographic distances. The divergence is only 0.55% over a 500 km distance between the Okavango Delta in Botswana and Bulawayo, Zimbabwe, and 1.35% for distances more than 1000 km between Okavango Delta, Botswana and Hotazel, South Africa (Bennett and Jarvis 2004). These low divergence values indicate a relatively recent and fast colonisation of the species' range, with a lack of significant landscape barriers preventing dispersal. Nevertheless, Van Daele et al. (2007) identified two genetically distinct groups, one comprising mole-rats from the regions of the Okavango, Bulawayo and Zambia, the other including individuals from Rundu (northern Namibia) and Dordabis in central Namibia.

Across its large geographical distribution, *F. damarensis* is also known to exhibit variability in pelage colour, morphology, growth rates, and group composition. While the majority of individuals are usually dark brown to black, a pale reddish-brown or 'fawn' colour phase occurs around Dordabis (Bennett and Jarvis 2004) and Rehoboth (N. C. Bennett, pers. obs.) in Namibia, and has also been observed in the Kgalagadi Transfrontier Park, South Africa (de Graaff 1972). In some cases, fur colouration can vary even within a single-family group (de Graaff 1972; N.C. Bennett, pers. obs.). The mean family size was found to be 8.7 with standard deviation (SD) 5.3 in Van Zylsrus, South Africa (Thorley et al. 2023); 6.3 (SD = 3.9) and 9.0 (SD = 5.3) in Tswalu, South Africa (Mynhardt et al. 2021, Finn 2017), and 10.4 (SD = 6.5) in Dordabis, Namibia (Bennett and Jarvis unpublished data). It should be mentioned that these three sites are situated at the southern and western periphery of the species' distribution range, and comparable data are lacking from the core and northeastern part of its geographic distribution. We expect that significant ecological variation occurs in these areas, as annual precipitation in the northern part of the distributional range is much more mesic and predictable (in the north it exceeds 1000 mm, compared to less than 200 mm in the south). Moreover, the Kalahari sands differ in origin, structure, and chemical composition (Garzanti et al. 2022) and the vegetation is markedly distinct (Ringrose et al. 2003) across the distributional range of *F. damarensis*, which likely results in substantial differences in available food resources.

Our aim in this study was to provide a comprehensive phylogeographic picture of *F. damarensis*. We analysed its intraspecific structure using one mitochondrial gene (cytochrome *b*, *CYTB*) and one nuclear gene (interphotoreceptor retinoid binding protein, *IRBP*). We obtained new fresh tissue samples, particularly from the northern part of its distribution area (Zambezi region), and genotyped museum material to substantially increase the geographic coverage of our data. Finally, to assess differentiation of the species across its large geographic distribution, we reviewed morphological characteristics of *F. damarensis*, together with climatic and soil characteristics from all localities and with available

genetic data. Although the primary focus of this study is on *F. damarensis*, we also analysed genetic diversity, historical demography and habitat characteristics of *F. micklemi*, its sister species. Given the phylogenetic proximity and parapatric distribution of these species, their comparison can be informative about factors behind the observed patterns.

Methods

Tissue samples

Mole-rats were collected by employing modified Hickmann traps and by using traditional capturing methods by local hunters. Captured animals were euthanized, tissue samples taken immediately and stored in 96% ethanol. Other tissues were contributed by natural history collections, namely Carnegie Museum of Natural History (CM) and Museum of Texas Tech University (TTU). DNA from all ethanol-preserved samples was extracted with the commercial isolation kit GeneJET Genomic DNA Purification Kit (Thermo Fisher Scientific) according to the enclosed protocol. In addition, we also analysed samples from museum voucher specimens, namely toe or skin clips kindly provided by the Field Museum of Natural History (FMNH), National Museum of Namibia (NMN), Natural History Museum of Zimbabwe (NMZB), and Museum of Comparative Zoology (MCZ). For the DNA isolation from these tissue samples the innuPREP Forensic Kit (Analytik Jena) was used.

Sanger and amplicon sequencing

Sanger sequencing was used to obtain *CYTB* (1140 bp) and *IRBP* (969 bp) from the ethanol-preserved tissues, using the same primers and PCR conditions as in Faulkes et al. (1997) and Bryja et al. (2014), respectively. The cleaned PCR products were commercially sequenced by the Genseq s.r.o. company. In museum tissues, DNA is typically degraded and we used amplicon sequencing on an Ilumina MiSeq platform (Ilumina, San Diego, CA, USA) to obtain short fragments of *CYTB*. For amplification we used two combinations of primers; Fuko_fw833_short: TAYGCYATYYTHCGATCYAT, Fuko_rev927_short: ATYATRCTKCGTTGYTTHGATG resulting in 74 bp long fragments, and L15411_modif: GA-YAAAATYYCHTTYCACCC, H15553_modif: GTAGGCRAAYAGGAARTATCA for 136 bp long fragments. Due to sequencing errors and cross-contamination, a heterogenous sample of sequence reads was obtained for each individual. We retained the most abundant haplotype in the sample, if it was abundant enough (at least 100 reads) and assigned to published *CYTB* sequences of *Fukomys* by the BLAST algorithm (Altschul et al. 1990). For the details of the preparation of sequencing libraries and the procedure of haplotypes assessment, see Šumbera et al. (2024). The sequencing was performed commercially at CEITEC (Masaryk University, Brno, Czech Republic).

Phylogenetic tree reconstruction

In total, we analysed *CYTB* sequences of 159 individuals from 65 localities across the distributional ranges of *F. damarensis* ($n=90$) and *F. micklemi* ($n=69$) (Fig. 1, Table S1). We used 59 published (Faulkes et al. 1997, 2004; Van Daele et al. 2007) and 100 unpublished sequences, including 33 sequences obtained from museum specimens. *IRBP* sequences (all of them unpublished) were obtained from 39 individuals, including two which were not represented in *CYTB* data set. The information about the individuals and their subsets used in various analyses is presented in Table S1. The newly obtained sequences are available under GenBank Accessions: PV756018–PV756117 (*CYTB*) and PV756118– PV756158 (*IRBP*).

Phylogenetic trees of both *CYTB* and *IRBP* sequences were estimated within a Bayesian framework using the software MrBayes 3.2.7a (Ronquist et al. 2012). Only subsets of data were used in these analyses: 98 unique *CYTB* haplotypes, each of them at least 600 bp long, and 27 unique *IRBP* sequences, representing diploid genotypes (i.e., with ambiguities in place of heterozygous positions). *Fukomys damarensis* was represented by 51 and 13 sequences in *CYTB* and *IRBP* tree, respectively. Both alignments also included two sequences of *F. mechowii* as outgroups (Table S1).

The nucleotide substitution model was pre-selected using ModelFinder tool (Kalyaanamoorthy et al. 2017) of IQ-TREE v. 2.1.3 (Nguyen et al. 2015) with all models available in MrBayes and all codon-position partitioning schemes considered. For the *CYTB* dataset, the best scheme was with the first two codon positions as one partition (with HKY+I substitution model) and the third codon position as another (with GTR+G). For the *IRBP* tree estimation, the alignment was partitioned by grouping the first and third codon positions together, while keeping the second codon position separate. The HKY model with equal rates across all sites was applied to both partitions. The substitution rates and transition/transversion rate ratios were allowed to vary between partitions. We ran four independent Markov chain Monte Carlo (MCMC) simulations for 2.5×10^6 generations of which every 1000^{th} generation was sampled, and their convergence was visually checked in Tracer 1.7 (Rambaut et al. 2018). The first 10% of posterior samples were discarded, while the rest were pooled and represented by the extended majority consensus tree with posterior mean branch lengths. The tree was then outgroup-rooted, and the outgroup was removed from it.

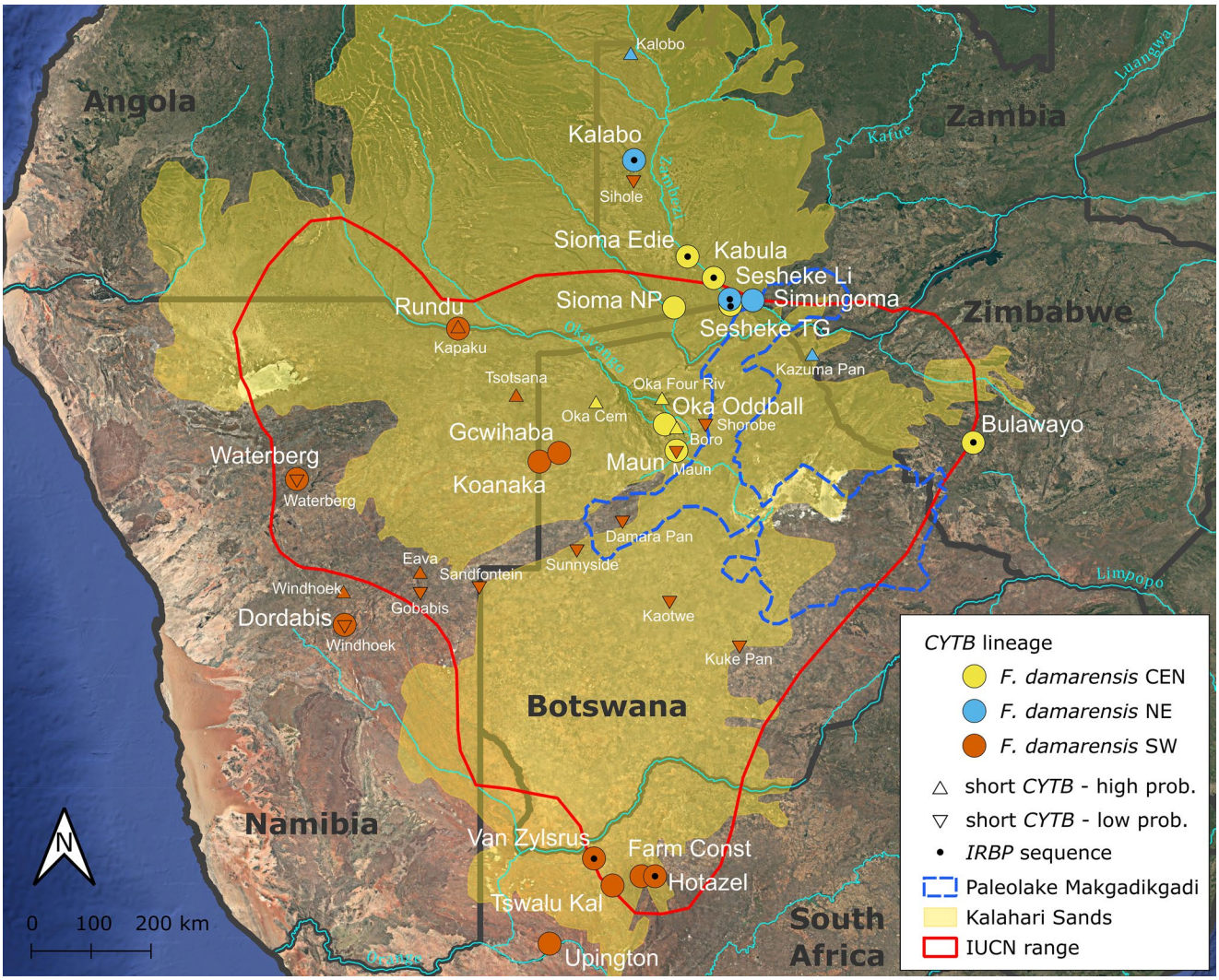

Fig. 1 Sampling sites of *F. damarensis* across its distributional range. The colours indicate three main mitochondrial lineages. Large circles are for long (≥ 700 bp) sequences, whereas small triangles represent short sequences, including those from museum voucher specimens. Triangles indicating sequences with low classification probabilities are oriented with their tip down. Black dots show sampling sites of *IRBP* sequenced individuals. In the background, the extent of Kalahari Sands and paleolake Magkadikgadi is depicted, together with the IUCN Red List (IUCN 2025) estimate of *F. damarensis*' distributional range

In the *CYTB* tree, main lineages were defined to describe its basic structure (see Results). The sequences not included in the tree (including the short ones) were assigned to the lineages using Evolutionary Placement Algorithm (EPA, Berger et al. 2011) implemented in RAxML 8.2.12 (Stamatakis 2014). Its results were summarized using the R package *epaclades*, available at https://github.com/onmikula/epaclades.

Bayesian skyline plot

Past population trends were estimated from *CYTB* alignments, separately for *F. damarensis* and *F. micklemi*, using Bayesian skyline coalescent model (Drummond et al. 2005) as implemented in BEAST 2 (Bouckaert et al. 2014). The model assumes data to come from a single panmictic population whose effective population size, and hence also coalescence time expectation, changes in piecewise manner in a small number of time segments (five in this case). The analysis keeps fixed the number of time segments, but not their sizes, defined as counts of the coalescence events they contain. It uses MCMC to sample from a joint posterior distribution of segment sizes, segment-specific population sizes, gene tree topologies and coalescent times. It outputs a posterior sample of trees and parameters, which are used to calculate marginal distributions of population sizes at a series of points back in time. Each analysis was run two times, the convergence was checked, and the samples pooled as before. The demographic curves, i.e., posterior distributions of population sizes and their summary

statistics, mean and 95% highest posterior density (HPD) intervals, were calculated in Tracer.

In order to put the estimated demographic curves on an explicit time scale, we used the estimated time of divergence between *F. damarensis* and *F. micklemi*, which is 780 ka (thousand years) before present (Šumbera et al. 2024, supplementary material). Given the average Kimura two-parameter (K2P) distance between *CYTB* sequences of these species (0.064), the mean substitution rate is 0.082/Ma. The branch lengths in the trees (originally in substitution units) were scaled by this value. In addition to the demographic curves, we also used the posterior samples to calculate extended majority consensus trees with posterior mean branch lengths for each species.

For Bayesian Skyline Plot analyses, we retained all unique long (>600 bp) haplotypes from each locality. In other words, when identical sequences were found at different localities, they were all retained as their occurrence is informative about population size. On the contrary, only one identical sequence per locality was included to avoid bias due to unequal sampling effort. The resulting numbers of sequences were 54 in *F. damarensis* and 51 in *F. micklemi*. None of the selected sequences was from the museum specimens, because these were ≤ 136 bp long and hence filtered out.

Distribution-wide ecological characteristics of *F. damarensis*

To assess the ecological differences among localities inhabited by *F. damarensis*, we conducted two separate Principal Component Analyses (PCA): one for climatic characteristics and another for soil properties. In both analyses, *F. micklemi* localities were included for comparison between habitats occupied by these two species. Climatic data, representing estimates for the past 100 years, were obtained from the CHELSA database (Karger et al. 2017, https://chelsa-climate.org). To characterize the climate of each locality, we used the full set of 19 BIOCLIM variables (Hijmans et al. 2005). Soil variable values were sourced from the SoilGrid™ database v. 2.0 (Poggio et al. 2021, http://www.soilgrids.org) and included the mass percentage of sand and clay, the volumetric percentage of coarse fragments, organic carbon content (g/kg), and soil bulk density (kg/dm^3), all estimated for a depth of 15–30 cm below surface. Response variables entering the analysis (climatic and soil parameters) were centred and standardized to have zero mean and unit variance. PCA was performed using the CANOCO5 software package (Šmilauer and Lepš 2014). The analysed datasets are available in Table S2.

We also made a compilation of information on body measurements, pelage coloration and habitat characteristics from 13 populations of *F. damarensis*, which were studied in detail (Table S3). One of them is reported here: we provide body measurements of 12 individuals recently collected in Zambia, an area from which such information was missing.

Results

Cytochrome *b* tree

The outgroup-rooted *CYTB* tree (Fig. 2A) showed *F. damarensis* was monophyletic with strong support (PP = 1.00) whereas the support for monophyly of *F. micklemi* was just moderate (PP = 0.87, Fig. 2A). Within *F. damarensis* we recognized three major lineages, labelled as "north-eastern" (NE), "central" (CEN) and "south-western" (SW). While the first two were monophyletic with strong support (PP = 1.00), the last one was monophyletic with weak support only (PP = 0.26). Whereas the first two lineages are located along the Zambezi River and Okavango Delta, with an extension to eastern Zimbabwe, the SW lineage has the broadest distribution across most of Botswana, South Africa and Namibia. Interestingly, one barcoded SW sample was found to occur in western Zambia (Figs. 1, 2B). The average K2P distances ($\hat{d}$) between the lineages were 0.016 (NE-SW), 0.016 (CEN-SW) and 0.014 (CEN-NE), respectively. The remaining 61 *CYTB* sequences, not included in the tree, were classified into these three lineages, usually with probabilities ≥ 0.90. Just 14 of the sequences were classified to SW lineage with probability = 0.48, either because they were short (originating from museum specimens) or due to weak separation of the lineages (Fig. 2A). However, their classification to SW makes sense geographically (cf. Fig. 1).

IRBP tree

In the IRBP tree (Fig. 3), only the monophyly of the two species was supported: moderately (PP = 0.69) in case of *F. damarensis*, strongly (PP = 1.00) in the case of *F. micklemi*. Otherwise, the topology of the tree was largely unresolved with most intraspecific nodes being supported with PP ≪ 0.50. In either of the species, however, there was no pattern apparent that would reflect the structure observed in the *CYTB* tree, as indicated by coloration of the tree tips.

Bayesian skyline plot

There was a large contrast between past population trends estimated for the two species (Fig. 4). While *F. damarensis* appeared to have undergone a fast population expansion in the recent past, the population size of *F. micklemi* was more stable over the covered period. The population size of

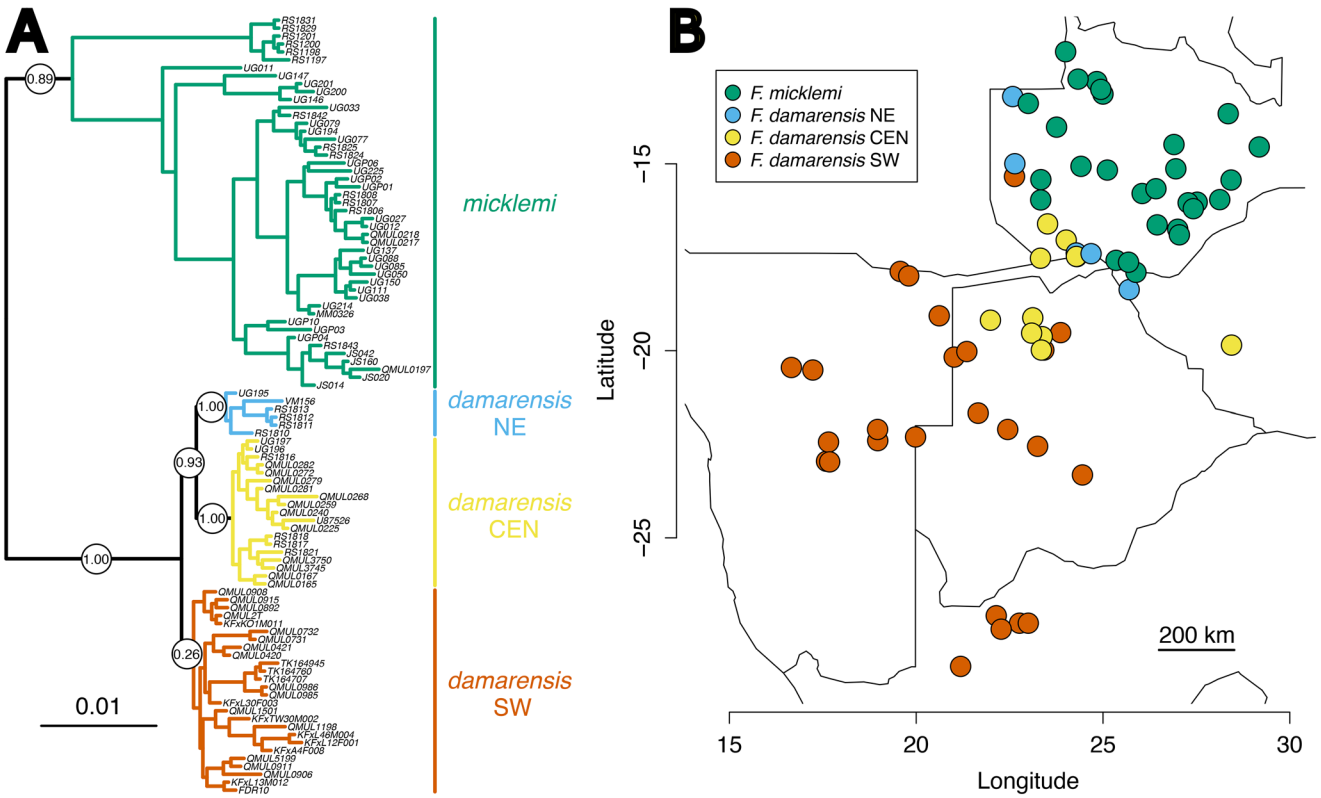

Fig. 2 (**A**) Cytochrome *b* tree and (**B**) distributional ranges of *F. damarensis* lineages (Northeastern - NE, Central - CEN, Southwestern - SW) and *F. micklemi*. Posterior probability values on the tree nodes are from MrBayes analysis

F. damarensis increased 5.4 times from 40 to 20 ka before present (BP) and even more (19.1 times) from 60 ka to the present. In contrast, the population of *F. micklemi* did not change more than 3.7 times in its size from the historical minimum (ca. 250 ka BP) to the maximum at present. The corresponding consensus trees differed accordingly (Fig. 5). The deepest coalescence dates back to 86 ka BP in *F. damarensis*, while 366 ka BP in *F. micklemi*. Interestingly, the monophyly of *F. damarensis* lineages was more strongly supported (PP ≥ 0.98) in this tree than in its outgroup-rooted MrBayes counterpart. The basal topology was unresolved, however, as the support for NE-SW sister relationship was weak (PP = 0.50).

Morphology of Zambian mole-rats

Out of 13 mole-rats collected in Zambia, we obtained body measurements for 12 individuals only. Mean body mass of males was 94.8 g (SD = 26.1 g, range = 71.0–136.3 g, $n = 5$) and 85.9 g (SD = 17.8 g, range: 54.2–108.2 g, $n = 6$) for females (see Table S3 for other body measurements). A swollen uterus and open vagina in the largest females indicate that they were sexually mature. The largest male (RS1817, body mass 136.2 g) had large testes (6.9 × 5.1 mm) and black perioral stains what might indicate it was the breeding male (Caspar et al. 2022). A single individual collected westerly from upper Zambezi in Kalabo, Zambia, was a large female weighing 149 g.

Ecological characteristics of *F. damarensis* across its area of distribution

The first two principal components (PC1 and PC2) derived from the analysis of soil variables together accounted for 70.8% of the total variation (Fig. 6A). PC1 (50.0%) primarily separated soils with higher clay and organic carbon content from those that are sandier and contain a greater proportion of coarse fragments. Along this gradient, both *F. micklemi* and *F. damarensis* occupy relatively broad ranges of soil types, with partial overlap between them. *Fukomys micklemi* is primarily associated with soils richer in organic carbon and clay, whereas *F. damarensis* – particularly its SW lineage – extends further into sandy and coarse-grained soils. The soils inhabited by the CEN and NE lineages largely overlap with those occupied by *F. micklemi*. PC2 (20.8%) further distinguished a subset of *F. damarensis* localities characterised by lighter soils (associated with lower bulk density), particularly near the Zambezi River and one site in the Okavango region (Fig. 6A).

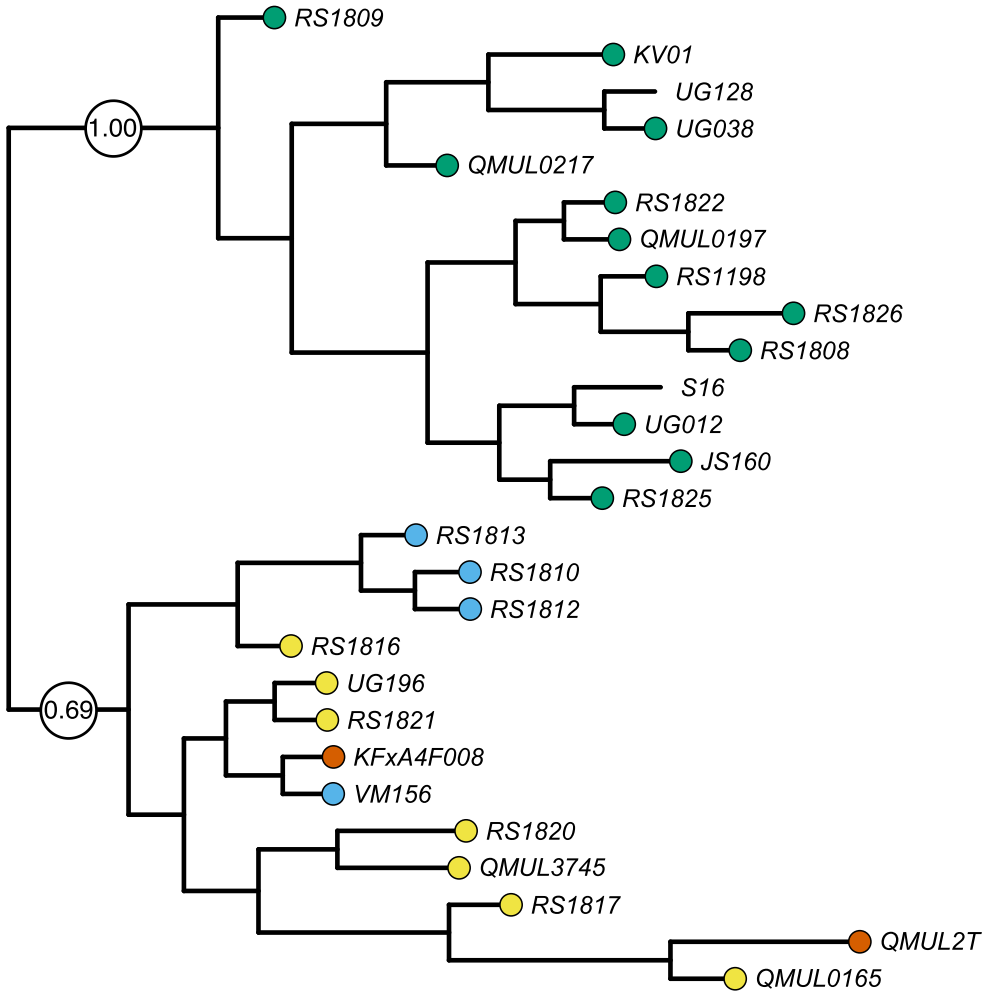

Fig. 3 Interphotoreceptor retinoid binding protein (*IRBP*) tree. The colours indicate which type of *CYTB*, as distinguished in MrBayes *CYTB* tree (Fig. 2A), the individuals were bearing. Posterior probabilities of species monophyly are on the tree nodes

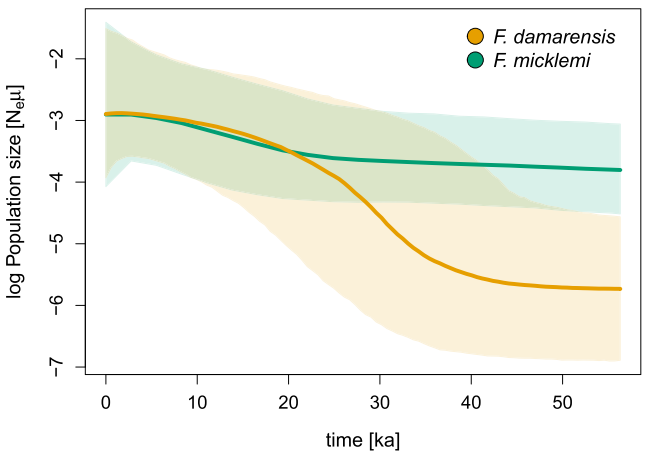

Fig. 4 Bayesian skyline plots showing the estimated past changes in effective population size. The solid lines are posterior means, the envelopes are 95% HPD intervals

Considering climatic parameters, the PC1 and PC2 together explained 78.8% of the total variation (Fig. 6B). On one extreme of PC1 (56.9%), there are localities characterised by high precipitation seasonality and generally wetter and warmer conditions – higher annual precipitation, higher precipitation during the wettest month and wettest quarter, as well as higher minimum and mean temperature during the coldest, driest month and quarter. This seasonality was characteristic for all localities of *F. micklemi* and the NE lineage of *F. damarensis*. The CEN lineage of *F. damarensis* occupies habitats with relatively low rainfall and temperatures. In contrast, most localities of SW lineage were found in areas with high diurnal and seasonal range of temperatures (high mean diurnal range, temperature seasonality, temperature annual range) and increased precipitation during the driest part of the year (precipitation of driest month and quarter, and coldest quarter). PC2 (21.9%) accounted for a trend within *F. micklemi* and SW lineage of *F. damarensis* (and also within CEN lineage due to an outlying record from Bulawayo, Zimbabwe). It captured a gradient of increasing temperatures, decreasing isothermality (i.e., ratio of daily and annual range of temperatures), and decreasing precipitation during the warmest quarter of the year (Fig. 6B).

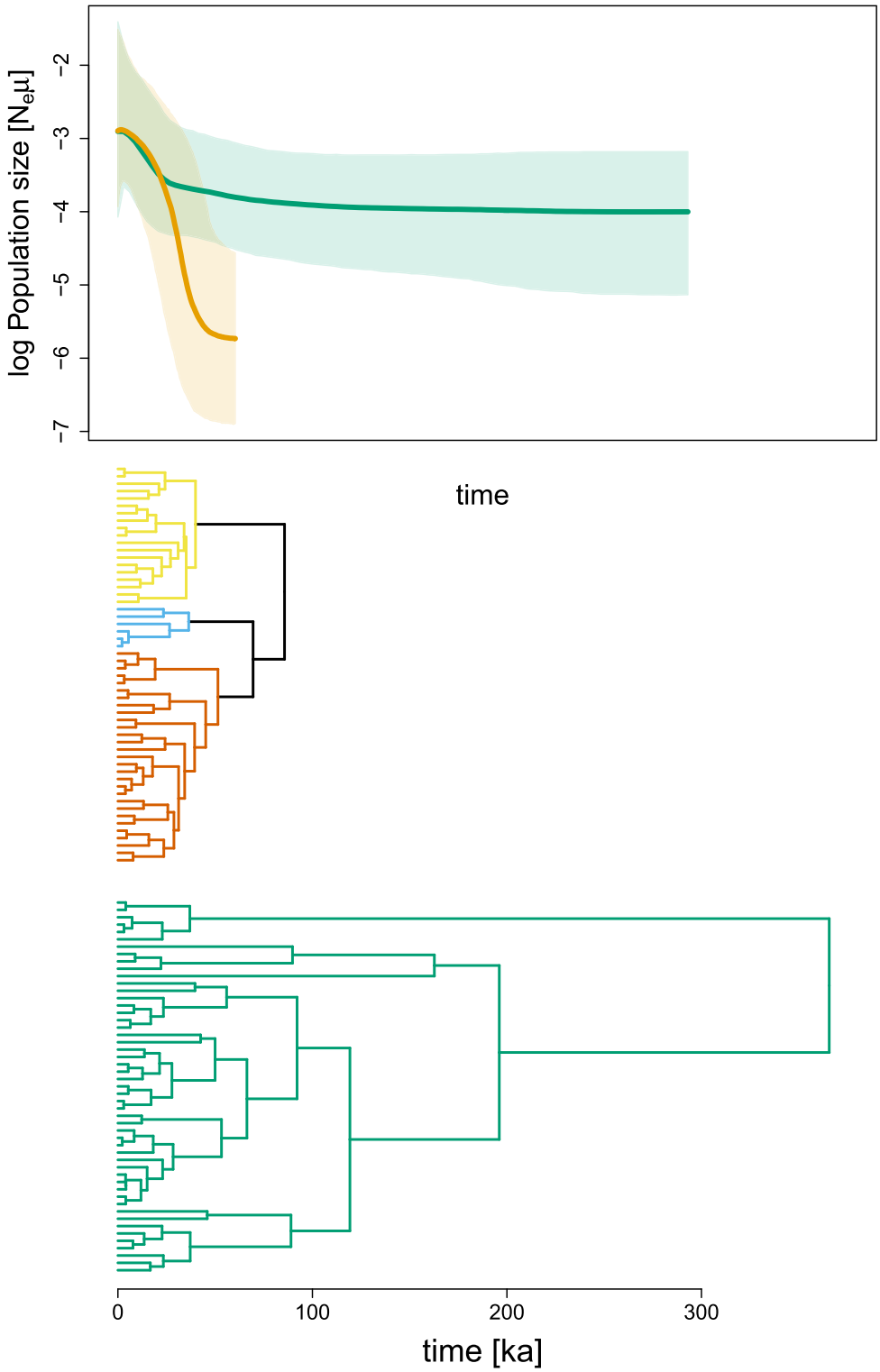

Fig. 5 Bayesian skyline plots and the corresponding consensus trees, all displayed on the shared time scale. In the consensus tree of *F. damarensis*, the colours indicate lineages distinguished in MrBayes *CYTB* tree (Fig. 2A), but the Bayesian skyline plot was estimated for the species as a whole

Discussion

In our study, we focused on intraspecific variation in a cooperatively breeding African mole-rat, *F. damarensis*. Although this species has been extensively studied for nearly four decades, surprisingly little is known about its intraspecific variation, particularly about its genetic differentiation across its broad geographic range. By combining *CYTB* sequences from fresh tissue samples and old museum samples, we were able to characterise the genetic variation of *F. damarensis* across its geographic distribution and to reconstruct the species' historical demography. The *CYTB*

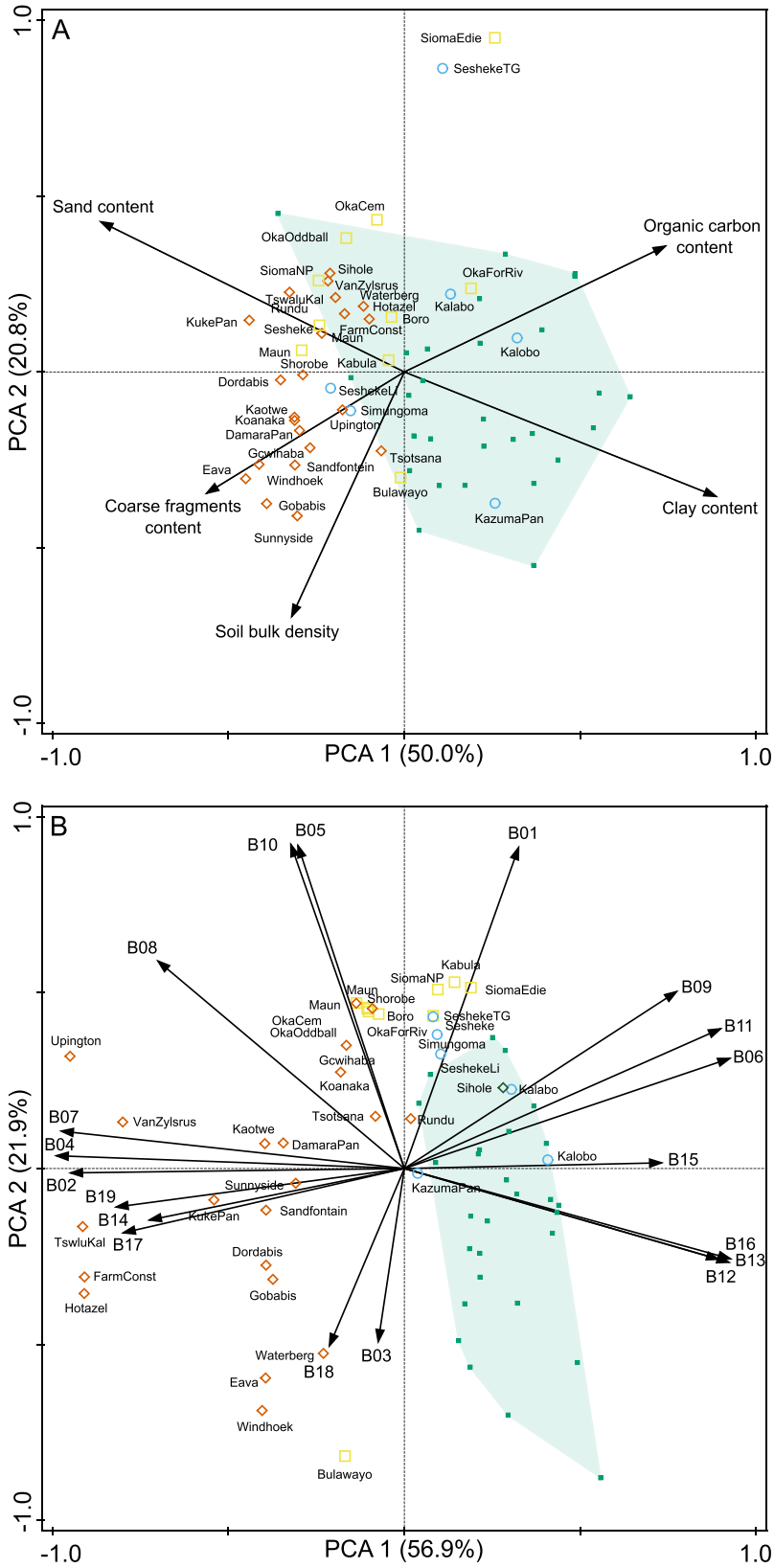

Fig. 6 Principal component analysis (PCA) plots illustrating interrelationships among (**A**) five soil characteristics and (**B**) 19 bioclimatic variables across localities inhabited by *F. micklemi* (green squares and polygon) and *F. damarensis*, represented by three lineages: SW lineage (orange diamonds), CEN lineage (yellow squares), NE lineage (blue circles). Bioclimatic variables include B1: annual mean temperature; B2: mean diurnal range (mean of monthly max temp: min temp); B3: isothermality (B2/B7) (*100); B4: temperature seasonality (standard deviation * 100); B5: max temperature of warmest month; B6: min temperature of coldest month; B7: temperature annual range (B5: B6); B8: mean temperature of wettest quarter; B9: mean temperature of driest quarter; B10: mean temperature of warmest quarter; B11: mean temperature of coldest quarter; B12: annual precipitation; B13: precipitation of wettest month; B14: precipitation of driest month; B15: precipitation seasonality (coefficient of variation); B16: precipitation of wettest quarter; B17: precipitation of driest quarter; B18: precipitation of warmest quarter; B19: precipitation of coldest quarter

phylogeny revealed the presence of three major matrilineages within *F. damarensis*. However, analysis of complete mitochondrial genomes would be necessary to resolve their relations and to conclusively test the monophyly of the SW lineage. The results of *CYTB* analyses were not fully conclusive as the basal topology was unresolved in both MrBayes and Bayesian Skyline Plot trees. In contrast to *CYTB* (i.e., mitochondrial) tree, the chosen nuclear marker (*IRBP*) supported only the split between *F. damarensis* and *F. micklemi* s.l., without revealing any intraspecific structure. This is not unexpected, given the relatively young age (86 ka) of the deepest coalescence in the *CYTB* tree and generally low mutation rates of nuclear genes.

Geographic distribution of CYTB variation in *F. damarensis*

At a broad geographic scale, the distributions of the three major *CYTB* lineages are intermingled (Fig. 2B). Two lineages occur in the broadly defined northern and central parts of the species' range: in the Zambezi region (NE) and from the Zambezi River southwards to the Okavango Delta and eastwards to Bulawayo in Zimbabwe (CEN). The southwestern lineage (SW) occupies a large area extending from central Namibia and northwestern South Africa through Botswana and into western Zambia. The monophyly of the SW lineage was supported only by the Bayesian skyline plot analysis, probably due to explicit modelling of population size changes, but even there the basal branching was unresolved. The SW lineage could be sister to NE+CEN (Fig. 2) or to NE alone (Fig. 5). In fact, individuals with different mitochondrial types were sampled in close proximity in some areas, namely in Northern Botswana (SW and NE), Okavango basin (SW and CEN) and around the Zambezi River (NE and CEN). Individuals of both the NE and CEN lineages were collected, for instance, in close vicinity of Sesheke, a small town on the north bank of the Zambezi (17°28'30"S, 24°17'30"E). Within the distribution of *F. damarensis*, the same co-occurrence of distinct mitochondrial lineages was observed in the pygmy mouse (*Mus minutoides*), namely in Koanaka Hills, northern Botswana (McDonough et al. 2013). We hypothesize this to be due to environmental stability of the area around the Upper Zambezi and Okavango basin, which supported long-term survival of mole-rat populations without severe bottlenecks and, thus, preservation of substantial genetic variability.

Similar to Van Daele et al. (2007), we collected *F. damarensis* from the left bank of the Zambezi River, where otherwise *F. micklemi* lives. Large rivers in the region may serve as major migration barriers to gene flow, as exemplified by the dichotomy of the pouched mouse *Saccostomus campestris campestris* from *S. c. mashonae* (Mikula et al. 2016; Krásová et al. 2021), divided by the Kafue and Zambezi rivers. Similar patterns have been observed in larger mammals (Cotterill 2003). However, some organisms with relatively low dispersal capacity have managed to overcome such barriers. Rather than actively crossing large rivers, mole-rats may have dispersed via local landscape connections that emerged due to very dynamic geomorphological processes during the late Pleistocene. During this period, the Zambezi River underwent significant reconfiguration and was even temporarily disconnected during the last glacial period (Moore et al. 2007). The mid-Zambezi was a discontinuous barrier in some periods, potentially allowing north-south mammalian migrations. Furthermore, repeated isolation and reconnection of mole-rat populations due to local shift of the river course may explain their presence on both banks. This process was proposed also to explain how the Mashona mole-rat *Fukomys darlingi* crossed the lower Zambezi and colonised southern Malawi (Šumbera et al. 2023).

Population expansion – the role of soils and climate

The most prominent finding of this study is the fast population expansion of *F. damarensis*. This is even more striking on the background of the demographic curve estimated for *F. micklemi* s.l., whose population has remained relatively stable over the past 300 ka. *Fukomys micklemi*, however, inhabits areas where vegetation and climate likely remained more stable over long periods. In contrast, the population expansion of *F. damarensis* was likely accompanied by a rapid range expansion, which is most clearly reflected in the large distribution of the SW lineage.

We assume that this population and range expansion of *F. damarensis* started from its core distribution area, where all major lineages are still present, namely, the region surrounding the Zambezi River and extending southwards toward the Okavango and Makgadikgadi pan. The persistence of both *F. damarensis* and *F. micklemi* in this area suggests that similar mesic conditions prevailing in this region were favourable for the long-term occurrence of both species, as also reflected in their spatial overlaps in climatic and soil variables (Fig. 6). Our PCA revealed that *F. damarensis* is predominantly restricted to coarse, sandy soils, whereas *F. micklemi* occupies primarily soils with higher clay and organic matter content. This pattern supports earlier findings that *F. damarensis* is closely associated with red Kalahari arenosols and other loose sandy substrates (Bennett and Jarvis 2004). Although the soil characteristics of habitats occupied by the three *F. damarensis* lineages partially overlap, a clear and gradual shift toward sandier soils is evident in the most widespread SW lineage. In contrast, individuals from the NE and CEN lineages occur in relatively less sandy soils (Fig. 6A).

These patterns partially align with Thorley et al. (2023), who analysed soil conditions at three sites (Kuruman River Reserve, Tswalu, and Dordabis) and found that these cluster near the centre of the multivariate environmental space. However, our results place these sites closer to the periphery of the species' actual distribution, likely because the north-eastern part of the range, where the NE and CEN lineages occur, was not included in their analysis.

In addition to substrate preferences, climatic conditions appear to have played an important role in the range dynamics of *F. damarensis*. During the last glacial maximum (25–15 ka), arid conditions (Beuning et al. 2011) promoted the accumulation of extensive sand deposits across central and southern Botswana (Munyikwa et al. 2000; Garzanti et al. 2022). Our analysis of georeferenced *CYTB* sequences suggests that the species may have originally evolved in areas with more consolidated soils — similar to those inhabited by *F. micklemi* — and subsequently colonised more arid and sandy environments. The availability of loose, easily excavated soils likely facilitated rapid expansion of *F. damarensis* across the Kalahari Basin.

Interestingly, the southwestern part of the species' range, where the SW lineage is dominant, is characterised by more extreme climatic conditions than those experienced by the NE and CEN lineages. This region receives lower and less seasonally predictable rainfall and is subject to more pronounced temperature fluctuations throughout the year (Fig. 6B; see also Thorley et al. 2023, supplementary material). Despite these environmental extremes, *F. damarensis* appears to cope well with such conditions. This ecological success was likely aided not only by the suitability of the sandy substrates but also by the species' notable dispersal capabilities, as individuals have been recorded moving over several kilometres (Finn et al. 2022).

Population expansion – spatiotemporal frame

Even if facilitated by environmental changes, the population expansion of *F. damarensis* was possible only once the new habitats became accessible due to the disappearance or overcoming of migration barriers. In the concerned area, large rivers and lakes, along with their associated swamps such as Makgadikgadi-Okavango palaeo-wetland (Fig. 1) likely acted as an important geographic barrier whose extent fluctuated on a millennial timescale (Burrough et al. 2009; Moore et al. 2012; Riedel et al. 2014). Mole-rats likely expanded into their current range only after these areas had dried up enough to become permeable to migration.

Although phylogeographic studies on small mammals distributed across the Kalahari sands remain scarce, the few available examples indicate significant population expansions similar to those of *F. damarensis*. Notably, signals of such expansions were detected in the bushveld gerbil (*Gerbilliscus leucogaster*) (McDonough et al. 2015) and the pouched mouse (*Saccostomus campestris*) (Mikula et al. 2016). These findings suggest that the spread of drier savannah habitats during glacial periods may have created suitable environments for *F. damarensis* and other xeric-adapted rodents. The Last Glacial Maximum (25–15 ka in this region) was characterised by the expansion of dry woodland and grassland habitats (Beuning et al. 2011), which may have simultaneously enhanced the availability of food resources on which mole-rats depend. Also, species distribution modelling shows that glacial conditions were more suitable for the pouched mouse than interglacial periods (Mikula et al. 2016). A similar pattern has been observed in giraffes, where the disappearance of the mega lake Makgadikgadi (16 ka before present, Riedel et al. 2014) facilitated their migration into the southern Kalahari region (Bock et al. 2014; Prochotta et al. 2024).

In this study, the expansion of *F. damarensis* was dated to 20–40 ka before present, and the expansions of *Gerbilliscus* and *Saccostomus* similarly arose around 40–50 ka (McDonough et al. 2015; Mikula et al. 2016). Dating of these expansions remains tentative, however, and is typically conditional on many assumptions. However, we consider it accurate enough to give us an idea about the timescale concerned. Our study did not estimate the age of the split between *F. damarensis* and *F. micklemi*, or divergence times between the lineages of *F. damarensis*. Such estimates made from our current data would require information we currently are not in possession of, namely precise estimates of *CYTB* mutation rate and generation time. Here, we used 0.78 Ma as the age of the *F. damarensis-micklemi* split, which was taken from our current estimate of time-calibrated mole-rat phylogeny (Šumbera et al. 2024, Supplementary material).

Karyotypic variation

There is no clear link between number of chromosomes and particular matrilineages of *F. damarensis*. All three known chromosome numbers 2n = 74, 78, 80 are present in the most widespread lineage SW (Nevo et al. 1986; Deuve et al. 2008). This is in line with low *CYTB* differentiation between populations of *F. micklemi* with 2n = 58 and 68 in central Zambia (Burda et al. 1999; Van Daele et al. 2004, this study) and implies little or no effect of these chromosomal changes on reproductive compatibility. Although less studied, only one cytotype (2n = 78) has been found so far in an area of two remaining matrilineages (NE and CEN) (Van Daele et al. 2004).

Morphological and life history differences

Similar to the findings of Van Daele et al. (2004), who reported black-furred *F. damarensis* individuals in Sioma Ngwezi, Zambia, we also observed very dark individuals around the Zambezi River. According to de Graaff (1972), *F. damarensis* is the only known species of the genus with pronounced adult colour polymorphism. De Graaff observed that reddish-brown individuals were found within the same family as dark slaty-grey and virtually black individuals in the Kgalagadi Transfrontier Park, South Africa. Nevertheless, remarkable interpopulation differences in fur colouration have also been described in *F. darlingi* (Šumbera et al. 2023) and are common in *F. micklemi*, where especially younger individuals can be very dark (our observation). Interestingly, dark pelage is atypical for mammals inhabiting arid environments, and is generally more common in species adapted to wetter conditions. This lead Roberts (1951) in de Graaff 1972) to speculate that dark colouration in *F. damarensis* may represent a retained ancestral trait from before the species radiated into desert environments. This interpretation aligns with the hypothesis that *F. damarensis* originated in a more humid northern environment before expanding into drier areas. Morphological adaptations to aridity have also been documented in the genus *Cryptomys*, the sister genus to *Fukomys*. Merchant et al. (2024) found significant morphological variation along an aridity gradient in *C. h. hottentotus*, with individuals from more arid regions exhibiting larger body sizes, larger spleens and kidneys, shorter legs, and greater inter-shoulder width.

Finn et al. (2018) found that body mass in *F. damarensis* may differ between populations: individuals in arid areas were heavier than those in areas with higher rainfall. Individuals in Dordabis, Namibia are heavier still, with some individuals approaching 300 g body mass (Bennett and Jarvis 2004). This has led authors to conclude that morphological differences are likely adaptations to local environmental conditions (soil hardness, food availability), and may be energy-saving mechanisms (Finn et al. 2018; Merchant et al. 2024). Although *F. damarensis* individuals newly sampled in Zambia, as well as those from Botswana (Smithers 1971), were generally smaller than those from other sites in South Africa and Namibia (see Table S3), we cannot yet attribute these differences to natural intraspecific variability and population-level divergence. Instead, the smaller body sizes observed in our sample may be an artifact of the trapping method used. Specifically, we primarily opportunistically collected individuals which entered the traps or visited burrow entrances first. In *Fukomys* mole-rats, including *F. damarensis*, it is known that non-reproductive individuals are more likely to be captured first, whereas the larger reproductive individuals tended to be captured later due to decreased out-of-nest activity (Voigt et al. 2019; Francioli et al. 2020; Zöttl et al. 2022). More systematic trapping efforts, particularly those targeting entire family groups, may provide a more representative information of body size variation across populations.

Conclusions and future perspectives

The results of our study indicate that the ancestral domain of the Damaraland mole-rat was located in the Upper Zambezi – Okavango Delta region, where all three matrilineages are present. Here, the climate is wetter and more predictable compared to the environments in which the species has been most extensively studied. Towards the end of the last glacial period, *F. damarensis* expanded southward and westward, coinciding with the aridification of the region, expansion of open habitats and shrinkage of wetlands that acted as major migration barriers before. For future research, it would be highly valuable to establish long-term research of *F. damarensis* in the northern part of its distribution, such as in Zambia or northern Botswana. Comparing population ecology, behaviour, and sociality in mole-rats from these more mesic environments, characterised by differing rainfall patterns and soil characteristics, with those from the most arid parts of the species' range could significantly enhance our understanding of their biology and sociality, as well as that of African mole-rats more broadly. This potential is underscored, for example, by the observation that one of the two families collected in the Okavango delta comprised 41 members (N.C. Bennett and C.G. Faulkes unpublished data, see also Table S3), representing the largest recorded family size for this species.

Supplementary information The online version contains supplementary material available at https://doi.org/10.1007/s42991-025-00546-3.

Acknowledgements For help during the field work we acknowledge V. Mazoch, H. Konvičková, J. Šklíba, J. Brabec, T. Nečas, J. Thorley, P. Vullioud, S. Bournbush, K. Flesness, J. Kjellberg Jensen, S. Kershenbaum, T. Manning, P. Majic, S. McGregor, A. Mitchell, J. Musafija, F. Santi, T. Waite, and A. Webb and all local collaborators. We thank T. Clutton-Brock, M. Manser, M. Zöttl, D. Gaynor, the Kalahari Research Trust and staff of the Kalahari Research Centre for their contributions to the field work in South Africa. We thank E. Oppenheimer & Son, D. McFadyen, G. van Dyk, and D. Smith for permission to conduct research at Tswalu Kalahari Reserve. We thank Jennifer Jarvis and Mike Griffin for assistance with field collections in Namibia and Botswana. We also thank curators, who helped us with access to museum collections, namely A. Fergusson (FMNH), H. Garner (TTU) and S. McLaren (CM). The assistance of C. Mateke (Livingstone Museum) with project logistics in Zambia was highly appreciated. For permission to carry out the research and to collect specimens in Zambia we are obliged to Ministry of Tourism (permit n. NPW 8/27/1) and to Office of Director of Forestry, Ministry of Green Economy and Environment (permit n. MGEE/FDHQ 101/19/22). We are grateful to the Northern Cape Department of Environment and Nature Conservation

for permission to conduct research in South Africa (permit 042/2013).

Author contributions R.Š. and O.M. initially conceived the research project. R.Š., M.U., N.C.B., S.J.E., C.G.F, K.T.F., M.L., K.P., P.A.A.G.D. and O.M. collected and/or provided tissue samples. The molecular work was performed by M.U. and B.Z. Phylogenetic data were analysed by O.M. and M.U. Ecological data were analysed by M.L. R.Š., M.U. and O.M. were primarily responsible for writing of the manuscript and contributed equally to this work.

Funding Open access publishing supported by the institutions participating in the CzechELib Transformative Agreement. This study was supported by the project of the Czech Science Foundation, n. GAČR, 20-10222S to RŠ and OM. Additional funding was provided by a British Ecological Society Grant to M. Zöttl and a European Research Council grant to T. Clutton-Brock (294494). NCB acknowledges the National Research Foundation, the National Geographic Society and the University of Pretoria for research grants to collect material and undertake research in Dordabis and Otjiwarongo in Namibia and Oddballs in the Okavango swamps in Botswana.

Data availability The datasets analysed in this study are available in the online Supplementary Information (Tables S1–S3) or in NCBI GenBank (https://www.ncbi.nlm.nih.gov/genbank).

Declarations

Compliance with ethical standards The study at the Kalahari Research Centre and Tswalu Kalahari Reserve was approved by the University of Pretoria animal ethics committee (EC032-13).

Conflicts of interest The authors have no competing interests to declare that are relevant to the content of this article.

References

Altschul SF, Gish W, Miller W, et al (1990) Basic local alignment search tool. J Mol Biol 215:403–410. https://doi.org/10.1016/S0022-2836(05)80360-2

Bennett NC, Faulkes CG (2000) African mole-rats: ecology and eusociality. Cambridge University Press, Cambridge

Bennett NC, Jarvis JU (2004) *Cryptomys damarensis*. Mamm Species 756:1–5. https://doi.org/10.2307/3504555

Berger SA, Krompass D, Stamatakis A (2011) Performance, accuracy, and web server for evolutionary placement of short sequence reads under maximum likelihood. Syst Biol 60:291–302. https://doi.org/10.1093/sysbio/syr010

Beuning KRM, Zimmerman KA, Ivory SJ, et al (2011) Vegetation response to glacial-interglacial climate variability near Lake Malawi in the southern African tropics. Palaeogeogr Palaeoclimatol Palaeoecol 303:81–92. https://doi.org/10.1016/j.palaeo.2010.01.025

Bock F, Fennessy J, Bidon T, et al (2014) Mitochondrial sequences reveal a clear separation between Angolan and South African giraffe along a cryptic rift valley. BMC Evol Biol 14:e219. https://doi.org/10.1186/s12862-014-0219-7

Bouckaert R, Heled J, Kühnert D, et al (2014) 2: a software platform for Bayesian evolutionary analysis. PLoS Comput Biol 10:e1003537. https://doi.org/10.1371/journal.pcbi.1003537

Bryja J, Mikula O, Šumbera R, et al (2014) Pan-African phylogeny of *Mus* (subgenus *Nannomys*) reveals one of the most successful mammal radiations in Africa. BMC Evol Biol 14:e256. https://doi.org/10.1186/s12862-014-0256-2

Buffenstein R, Park TJ, Holmes MM (2021) The extraordinary biology of the naked mole-rat. In: Book series: Advances in experimental medicine and biology. Springer, Cham. https://doi.org/10.1007/978-3-030-65943-1

Burda H, Zima J, Scharff A, et al (1999) The karyotypes of *Cryptomys anselli* sp. nova and *Cryptomys kafuensis* sp. nova: new species of the common mole-rat from Zambia (Rodentia, Bathyergidae). Z Säugetierkd 64:36–50

Burrough SL, Thomas DSG, Bailey RM (2009) Mega-lake in the Kalahari: a late Pleistocene record of the palaeolake Makgadikgadi system. Quat Sci Rev 28:1392–1411. https://doi.org/10.1016/J.QUASCIREV.2009.02.007

Caspar KR, Stopka P, Issel D, et al (2022) Perioral secretions enable complex social signaling in cooperatively-breeding mole-rats (genus *Fukomys*). Sci Rep 12:22366. https://doi.org/10.1038/s41598-022-26351-3

Cotterill FPD (2003) Geomorphological influences an Vicariant evolution in some African mammals in the Zambezi basin: some lessons for conservation. In: Plowman A (ed) Ecology and conservation of mini-antelope: Proceedings of an International Symposium on Duiker and Dwarf Antelope in Africa. Filander Verlag, Fürth, pp 11–58

de Graaff G (1972) On the mole-rat (*Cryptomys hottentotus damarensis*) (Rodentia) in the Kalahari Gemsbok National Park. Koedoe 15:25–35. https://doi.org/10.4102/koedoe.v15i1.665

Deuve JL, Bennett NC, Britton-Davidian J, et al (2008) Chromosomal phylogeny and evolution of the African mole-rats (Bathyergidae). Chromosome Res 16:57–74. https://doi.org/10.1007/s10577-007-1200-8

Drummond AJ, Rambaut A, Shapiro B, et al (2005) Bayesian coalescent inference of past population dynamics from molecular sequences. Mol Biol Evol 22:1185–1192. https://doi.org/10.1093/molbev/msi103

Fang X, Seim I, Huang Z, et al (2014) Adaptations to a subterranean environment and longevity revealed by the analysis of mole rat genomes. Cell Rep 8:1354–1364. https://doi.org/10.1016/j.celrep.2014.07.030

Faulkes CG, Abbott DH, Hp O, et al (1997) Micro-and macrogeographical genetic structure of colonies of naked mole-rats *Heterocephalus glaber*. Mol Ecol 6:615–628. https://doi.org/10.1046/j.1365-294x.1997.00227.x

Faulkes CG, Bennett NC (2021) Social evolution in African mole-rats – a comparative overview. In: Buffenstein R, Park T, Holmes M (eds) The extraordinary biology of the naked mole-rat. Advances in experimental medicine and biology. Springer, Cham, pp 1–33. https://doi.org/10.1007/978-3-030-65943-1_1

Faulkes CG, Bennett NC, Bruford MW, et al (1997) Ecological constraints drive social evolution in the African mole–rats. Proc R Soc Lond B 264:1619–1627. https://doi.org/10.1098/rspb.1997.0226

Faulkes CG, Verheyen E, Verheyen W, et al (2004) Phylogeographical patterns of genetic divergence and speciation in African mole-rats (family: Bathyergidae). Mol Ecol 13:613–629. https://doi.org/10.1046/j.1365-294X.2004.02099.x

Finn KT (2017) Density-dependent effects on body size, philopatry, and dispersal in Damaraland mole-rats (Fukomys damarensis) [master's thesis]. [Makhanda (Eastern Cape province, RSA)]: Rhodes University. http://hdl.handle.net/10962/50495

Finn KT, Parker DM, Bennett NC, et al (2018) Contrasts in body size and growth suggest that high population density results in faster pace of life in Damaraland mole-rats (*Fukomys damarensis*). Can J Zool 96:920–927. https://doi.org/10.1139/cjz-2017-0200

Finn KT, Thorley J, Bensch HM, et al (2022) Subterranean life-style does not limit long distance dispersal in African mole-rats. Front Ecol Evol 10:879014. https://doi.org/10.3389/fevo.2022.879014

Francioli Y, Thorley J, Finn K, et al (2020) Breeders are less active forager than non-breeders in wild Damaraland mole-rats. Biol Lett 16:20200475. https://doi.org/10.1098/rsbl.2020.0475

Garzanti E, Pastore G, Stone A, et al (2022) Provenance of Kalahari Sand: paleoweathering and recycling in a linked fluvial-aeolian system. Earth Sci Rev 224:103867. https://doi.org/10.1016/j.earscirev.2021.103867

Happold DCD (2013) Mammals of Africa - volume iii: rodents, hares and rabbits. Bloomsbury Publishing, London

Hijmans RJ, Cameron SE, Parra JL, Jones PG, Jarvis A (2005) Very high resolution interpolated climate surfaces for global land areas. Int J Climatol 25:1965–1978. https://doi.org/10.1002/joc.1276

IUCN (2025) The IUCN red list of threatened species. Version 2025-1. Accessed 1 Feb 2025 https://www.iucnredlist.org.

Jarvis JUM, Bennett NC (1993) Eusociality has evolved independently in two genera of bathyergid mole-rats – but occurs in no other subterranean mammal. Behav Ecol Sociobiol 33:353–360. https://doi.org/10.1007/BF02027122

Kalyaanamoorthy S, Minh BQ, Wong TKF, et al (2017) ModelFinder: fast model selection for accurate phylogenetic estimates. Nat Methods 14:587–589. https://doi.org/10.1038/nmeth.4285

Karger DN, Conrad O, Böhner J, et al (2017) Climatologies at high resolution for the earth's land surface areas. Sci Data 4:170122. https://doi.org/10.1038/sdata.2017.122

Krásová J, Mikula O, Bryja J, et al (2021) Biogeography of Angolan rodents: the first glimpse based on phylogenetic evidence. Divers Distrib 27:2571–2583. https://doi.org/10.1111/ddi.13435

McDonough MM, Sotero-Caio CG, Ferguson AW, et al (2013) Mitochondrial DNA and karyotypic data confirm the presence of *Mus indutus* and *Mus minutoides* (Mammalia, Rodentia, Muridae, *Nannomys*) in Botswana. Zookeys 359:51. https://doi.org/10.3897/zookeys.359.6247

McDonough MM, Šumbera R, Mazoch V, et al (2015) Multilocus phylogeography of a widespread savanna-woodland-adapted rodent reveals the influence of Pleistocene geomorphology and climate change in Africa's Zambezi region. Mol Ecol 24:5248–5266. https://doi.org/10.1111/mec.13374

Merchant HN, Portugal SJ, Bennett NC, et al (2024) New insights into morphological adaptation in common mole-rats (*Cryptomys hottentotus hottentotus*) along an aridity gradient. Ecol Evol 14:e11301. https://doi.org/10.1002/ece3.11301

Mikula O, R Š, Aghová T, et al (2016) Evolutionary history and species diversity of African pouched mice (Rodentia: Nesomyidae: *Saccostomus*). Zool Scr 45:595–617. https://doi.org/10.1111/zsc.12179

Šmilauer P, Lepš J (2014) Multivariate analysis of ecological data using Canoco 5. Cambridge University Press, Cambridge

Monadjem A, Taylor PJ, Denys C, et al (2015) Rodents of sub-Saharan Africa: a biogeographic and taxonomic synthesis. De Gruyter, Berlin, München, Boston. https://doi.org/10.1515/9783110301915

Moore AE, Cotterill FPD, Main MPL, et al (2007) The Zambezi River. In: Gupta A (ed) Large rivers: geomorphology and management. John Wiley & Sons, Chichester, pp 311–332. https://doi.org/10.1002/9780470723722.ch15

Moore JM, Polteau S, Armstrong RA, et al (2012) The age and correlation of the postmasburg group, southern Africa: constraints from detrital zircon grains. J Afr Earth Sci 64:9–19. https://doi.org/10.1016/j.jafrearsci.2011.11.001

Munyikwa K, Van Den Haute P, Vandenberghe D, et al (2000) The age and palæoenvironmental significance of the Kalahari Sands in western Zimbabwe: a thermoluminescence reconnaissance study. J Afr Earth Sci 30:941–956. https://doi.org/10.1016/S0899-5362(00)00062-2

Mynhardt S, Harris-Barnes L, Bloomer P, et al (2021) Spatial population genetic structure and colony dynamics in Damaraland mole-rats (*Fukomys damarensis*) from the southern Kalahari. BMC Ecol Evol 21:221. https://doi.org/10.1186/s12862-021-01950-2

Nevo E, Capanna E, Corti M, et al (1986) Karyotype differentiation in the endemic subterranean mole rats of South Africa (Rodentia, Bathyergidae). Z Säugetierkd 51:36–49.

Nguyen LT, Schmidt HA, Von Haeseler A, et al (2015) IQ-TREE: a fast and effective stochastic algorithm for estimating maximum-likelihood phylogenies. Mol Biol Evol 32:268–274. https://doi.org/10.1093/molbev/msu300

Poggio L, de Sousa Lm, Batjes NH, et al (2021) SoilGrids 2.0: producing soil information for the globe with quantified spatial uncertainty. SOIL 7:217–240. https://doi.org/10.5194/soil-7-217-2021

Prochotta D, Winter S, Fennessy J, et al (2024) Population genomics of the southern giraffe. Mol Phylogenet Evol 201:108198. https://doi.org/10.1016/j.ympev.2024.108198

Rambaut A, Drummond AJ, Xie D, et al (2018) Posterior summarization in Bayesian phylogenetics using Tracer 1.7. Syst Biol 67:901–904. https://doi.org/10.1093/sysbio/syy032

Riedel F, Henderson ACG, K-U H, et al (2014) Dynamics of a Kalahari long-lived mega-lake system: hydromorphological and limnological changes in the Makgadikgadi Basin (Botswana) during the terminal 50 ka. Hydrobiologia 739:25–53. https://doi.org/10.1007/s10750-013-1647-x

Ringrose S, Matheson W, Wolski P, et al (2003) Vegetation cover trends along the Botswana Kalahari transect. J Arid Environ 54:297–317. https://doi.org/10.1006/jare.2002.1092

Roberts A (1951) The mammals of South Africa. The Trustees of the Mammals of South Africa Book Fund , Johannesburg.

Ronquist F, Teslenko M, Van Der Mark P, et al (2012) Mrbayes 3.2: efficient Bayesian phylogenetic inference and model choice across a large model space. Syst Biol 61:539–542. https://doi.org/10.1093/sysbio/sys029

Smithers RHN (1971) Mammals of Botswana. University of Pretoria, Pretoria

Stamatakis A (2014) RAxML version 8: a tool for phylogenetic analysis and post-analysis of large phylogenies. Bioinformatics 30:1312–1313. https://doi.org/10.1093/bioinformatics/btu033

Thorley J, Bensch HM, Finn K, et al (2023) Damaraland mole-rats do not rely on helpers for reproduction or survival. Evol Lett 7:203–215. https://doi.org/10.1093/evlett/qrad023

Šumbera R, Uhrová M, Begall S, et al (2023) The biology of an isolated Mashona mole-rat population from southern Malawi, with implications for the diversity and biogeography of the genus *Fukomys*. Org Divers Evol 23:603–620. https://doi.org/10.1007/s13127-023-00604-z

Šumbera R, Uhrová M, Montoya-Sanhueza G, et al (2024) Genetic diversity of the largest African mole-rat genus, *Bathyergus*. One, two or four species? Mol Phylogenet Evol 199:108157. https://doi.org/10.1016/j.ympev.2024.108157

Van Daele PAAG, Dammann P, Meier JL, et al (2004) Chromosomal diversity in mole-rats of the genus *Cryptomys* (Rodentia: Bathyergidae) from the Zambezian region: with descriptions of new karyotypes. J Zool 264:317–326. https://doi.org/10.1017/S0952836904005825

Van Daele PAAG, Verheyen E, Brunain M, et al (2007) Cytochrome b sequence analysis reveals differential molecular evolution in African mole-rats of the chromosomally hyperdiverse genus *Fukomys* (Bathyergidae, Rodentia) from the Zambezian region. Mol Phylogenet Evol 45:142–157. https://doi.org/10.1016/j.ympev.2007.04.008

Voigt C, ter Maat A, Bennett NC (2019) No evidence for multimodal body mass distributions and body mass-related capture order in wild-caught Damaraland mole-rats. Mamm Biol 95:123–126. https://doi.org/10.1016/j.mambio.2018.09.012

Wong HS, Freeman DA, Zhang Y (2022) Not just a cousin of the naked mole-rat: Damaraland mole-rats offer unique insights into biomedicine. Comp Biochem Physiol B Biochem Mol Biol 262. https://doi.org/10.1016/j.cbpb.2022.110772

Young AJ, Jarvis JUM, Barnaville J, et al (2015) Workforce effects and the evolution of complex sociality in wild Damaraland mole-rats. Am Nat 186:302–311. https://doi.org/10.1086/682048

Zöttl M, Bensch HM, Finn KT, et al (2022) Capture order across social bathyergids indicates similarities in division of labour and spatial organisation. Front Ecol Evol 10:877221. https://doi.org/10.3389/fevo.2022.877221